Enteroaggregative *Escherichia coli* Disrupts Epithelial Cell Tight Junctions[▽]

Maura C. Strauman,[1] Jill M. Harper,[2] Susan M. Harrington,[3]
Erik Juncker Boll,[4] and James P. Nataro[2]*

*The Wistar Institute, Philadelphia, Pennsylvania[1]; Center for Vaccine Development; Departments of Pediatrics and Medicine,
University of Maryland School of Medicine, Baltimore, Maryland[2]; Department of Pathology and Laboratory Medicine,
Albany Medical Center, Albany, New York[3]; and Department of Microbiological Surveillance and Research,
Statens Serum Institut, Copenhagen, Denmark[4]*

Enteroaggregative *Escherichia coli* (EAEC) is responsible for inflammatory diarrhea in diverse populations, but its mechanisms of pathogenesis have not been fully elucidated. We have used a previously characterized polarized intestinal T84 cell model to investigate the effects of infection with EAEC strain 042 on tight junction integrity. We find that infection with strain 042 induces a decrease in transepithelial electrical resistance (TER) compared to uninfected controls and to cells infected with commensal *E. coli* strain HS. When the infection was limited after 3 h by washing and application of gentamicin, we observed that the TER of EAEC-infected monolayers continued to decline, and they remained low even as long as 48 h after the infection. Cells infected with the afimbrial mutant strain 042*aafA* exhibited TER measurements similar to those seen in uninfected monolayers, implicating the aggregative adherence fimbriae II (AAF/II) as necessary for barrier dysfunction. Infection with wild-type strain 042 induced aberrant localization of the tight junction proteins claudin-1 and, to a lesser degree, occludin. EAEC-infected T84 cells exhibited irregular shapes, and some cells became elongated and/or enlarged; these effects were not observed after infection with commensal *E. coli* strain HS or 042*aafA*. The effects on tight junctions were also observed with AAF/I-producing strain JM221, and an afimbrial mutant was similarly deficient in inducing barrier dysfunction. Our results show that EAEC induces epithelial barrier dysfunction *in vitro* and implicates the AAF adhesins in this phenotype.

Enteroaggregative *Escherichia coli* (EAEC) causes inflammatory, watery diarrhea in diverse clinical settings (14, 15). An epidemiologic study conducted in Baltimore, MD, and New Haven, CT, found that EAEC was the most frequent bacterial pathogen occurring in patients with diarrhea across all ages (27).

The pathogenesis of EAEC infection is thought to comprise adherence to the intestinal mucosa, followed by release of cytotoxins and enterotoxins. Adherence of EAEC to human intestinal explants is mediated by the aggregative adherence fimbriae (AAF), which are related to the Dr adhesins of diarrheagenic and uropathogenic *E. coli* (25). Prototype EAEC strain 042, shown to produce diarrhea in adult volunteers, exhibits the AAF/II variant, the expression of which requires a XylS/AraC family regulator called AggR (11). AAF genes and AggR are encoded on the 60-to 65-MDa EAEC virulence plasmid designated pAA (24, 25). This plasmid in strain 042 is specifically designated pAA2. We have recently shown that AggR also activates a large number of additional genes on plasmid pAA and on the EAEC chromosome (N. Morin and J. P. Nataro, unpublished data). Chief among the chromosomally encoded genes of the AggR regulon are those encoding a type VI secretion system designated the *aai* genes. The contribution of the *aai* locus remains unknown.

Clinical and laboratory data suggest that EAEC induces an inflammatory enteritis (14, 24). Studies using nonpolarized T84 and HT-29 cells implicated the 042 flagellin subunit FliC, which is not under the control of AggR, as the major inducer of interleukin 8 (IL-8) release (41). However, in polarized T84 monolayers, factors under the control of AggR also contribute to IL-8 release, and full IL-8 induction requires the AAF/II adhesin (15).

Many bacterial enteric pathogens that induce IL-8 release also cause a reduction in transepithelial electrical resistance (TER) in polarized epithelial cells. Disruption of epithelial barrier function may lead directly to secretion of fluid and electrolytes (the "leak-flux" model [22, 35, 39]), may contribute to mucosal protein loss and malabsorption, and may also facilitate access to the basolateral compartment by pathogens that prefer this route of entry. Herein we report that EAEC induces persistent loss of epithelial integrity accompanied by delocalization of tight junction proteins, effects that require expression of the AAF/II adhesin.

MATERIALS AND METHODS

Bacterial strains and infection. Bacterial strains used in this work are listed in Table 1. Prototype EAEC strains included AAF/II-producing strain 042 and AAF/I-producing strain JM221. Natural commensal nonpathogenic *E. coli* strain HS was used as a negative control for all studies. Bacteria were routinely cultured on Luria-Bertani (LB) agar and in LB broth containing the following concentrations of antibiotics where appropriate: 50 μg/ml kanamycin, 100 μg/ml streptomycin, and 60 μg/ml ampicillin. For polarized T84 cell experiments, strains were grown in LB broth overnight at 37°C in static conditions with appropriate antibiotic selection to retain plasmids. Prior to infection, bacteria were subcultured into Dulbecco's modified eagle medium (DMEM) containing 0.45% glucose with the appropriate antibiotic as previously described (15).

The AAF/I gene cluster (*aggDCBA*) in JM221 was deleted by allelic exchange with a kanamycin resistance-encoding cassette flanked by regions homologous to sequences on either side of the AAF/I gene cluster. The cassette was generated by using a previously described three-step PCR procedure (8, 42). In the first step, the kanamycin resistance-encoding gene (*kan*) was amplified from pKD4 using primers Kn1 (5′-GTGTAGGCTGGAGCTGCTTC-3′) and Kn2 (5′-ATGGGAATTAGCC

* Corresponding author. Mailing address: 685 W. Baltimore St., Baltimore, MD 21201. Phone: (410) 706-5328. Fax: (410) 706-6205. E-mail: jnataro@medicine.umaryland.edu.

TABLE 1. Bacterial strains used in this study

Strain	Characteristic(s)[a]	Source or reference
042	Archetype EAEC strain expressing AAF/II (serotype 044:H18); Sm, Tc, Cm	26
JM221	AAF/I producing archetype EAEC strain	26
JM221*agg*	JM221 in which a kanamycin cassette was inserted into the *aggDBCA* cluster; Kan	E. J. Boll and B. A. McCormick, unpublished data
Salmonella sp. CS401	Clinical isolate of *Salmonella enterica* serovar Typhimurium	31
042*fliC*	042 with suicide plasmid pJP5603 inserted into the gene *fliC*; Km	41
042*aggR*	042 with pJP5603 inserted into the gene *aggR*	28
042*aggR* (pBAD*aggR*)	042*aggR* complemented with *aggR* cloned downstream of the *ara* promoter in pBAD30; Km	37
042*aafA* 3.4.14	042 with Tn*phoA* inserted into *aafA*, inactivating AAF/II expression; no fimbriae produced; Km	7
042*aafA* 2.94	042 with Tn*phoA* inserted into *aafA*; defective nonadherent fimbriae produced; Km	7
042*aafB*	042 with JP5603 inserted into *aafB*; afimbriate; Km	11
042*aafC*	042 with Km marker inserted into *aafC*; afimbriate; Km	10
042*pet-astA*	042 in which the genes encoding *pet* and *astA* have been deleted; Km	E. Lim and J. P. Nataro, unpublished
HS	Human commensal *E. coli* strain, nonpathogenic in volunteers; Nal	20
HS(pAA2)	HS transformed with pAA2 containing insertion into a silent locus; Km	14

[a] Sm, streptomycin resistant; Tc, tetracycline resistant; Cm, chloramphenicol resistant; Nal, nalidixic acid resistant.

ATGGTCC-3′). A 373-bp region and a 249-bp region flanking the AAF/I gene cluster were PCR amplified using the primer sets B-*aagD*-F (5′-TTTTTAGCGTT ATATGATTTGA-3′) and B-*aggD*-R (5′-GAAGCAGCTCCAGCCTACACAGG CGGCTTGATTGTAGAG-3′) and E-*aggA*-F (5′-GGACCATGGCTAATTCCCA TATTTATGCATTACTTTGGGTTTAG-3′) and E-*aggA*-R (5′-ACCTGTTCCCC ATAACCAGACC-3′). The primers contained 20-bp regions homologous to 5′ and 3′ termini of the gene *kan*. The flanking regions were added onto each side of the gene *kan* by PCR amplification using B-*aagD*-F and E-*aggA*-R. The purified PCR products were electroporated into JM221 harboring the thermosensitive plasmid pKOBEGApra encoding the λRed recombinase. Both mutants were selected by growth on LB plates containing 25 μg/ml kanamycin at 37°C. Loss of the pKOBEGApra plasmid was verified by the inability of the mutants to grow on LB plates containing 30 μg/ml apramycin. Correct allelic exchange was verified by PCR analysis using combinations of primers inside the gene *kan* (K1 [5′-CAG TCATAGCCGAATAGCCT-3′] and K2 [5′-CGGTGCCCTGAATGAACTGC-3′]) and primers B-*aagD*-F and E-*aggA*-R (5′-ACCTGTTCCCCATAACCAGA CC-3′). To verify that the JM221*aggR* does not express fimbriae, the mutant was analyzed for the ability to agglutinate human and sheep erythrocytes.

A region of the virulence plasmid of strain 042 (previously designated pAA2) containing the adjacent genes *pet* and *astA* (encoding the EAST1 toxin) was deleted by using suicide vector pCVD442 as described previously (9). The deletion was constructed using overlapping primers with the following sequences: 5′-TTGGCG TTGATACCGAGAGGC-3′ with XbaI-SalI ends; and 5′-AAACAGCAATGAGTC CGCCA, 5′-CAGTCAGCACATTGAGCCAG, and 5′-TCTGGCCACTCTGATA CCTT-3′ with SalI-SphI ends. The resulting fragments were digested with SalI, ligated, and cloned into pCVD442.

Cell culture. Human colonic T84 intestinal epithelial cells (ATCC CCL-248) were routinely maintained in DMEM–F-12 media (Invitrogen) containing 10% fetal bovine serum (Sigma), 50 U ml^{-1} penicillin, and 50 mg ml^{-1} streptomycin. Polarized T84 cell monolayers were generated as previously described. Briefly, T84 cells between passages 8 and 20 were seeded at a density of 3×10^5 cells/ml onto collagen-coated, 12-mm polycarbonate Transwell permeable support cell culture inserts (0.4 μm pore size; Costar) and grown for 10 to 14 days, during which time the cells were fed daily. Monolayer resistance was determined using an EVOM ohmmeter with the Endohm 12 and STX2 electrodes (World Precision Instruments, Inc.). Monolayers were considered polarized when resistance was equal to or greater than 1,000 Ω/cm^2 and not more than 3,000 Ω/cm^2. Background resistance from collagen-coated, cell-free membranes was subtracted from initial resistance values in order to obtain resistance values used in statistical analyses (discussed below).

One hour before infection, polarized T84 cells were washed three times with phosphate-buffered saline (PBS) or Hanks' balanced salt solution (HBSS) to remove fetal bovine serum (FBS) and antibiotics. Fresh DMEM–F-12 containing 1% methyl-α-D-mannopyranoside (mannose) was then added to apical and basolateral compartments, and cells were equilibrated at 37°C in 5% CO$_2$ for 30 to 60 min. Overnight cultures of bacteria were standardized in DMEM-high glucose (HG) to an optical density at 600 nm (OD$_{600}$) of 0.30 ± 0.02, which is equal to approximately 2×10^8 to 4×10^8 CFU/ml. Mannose was added to each culture to a concentration of 1%.

For each sample, 100 μl of culture (MOI, ~10) was added to the apical side of three separate wells. DMEM-HG–1% mannose was added to uninfected wells and the well with no cells. The infected cells were incubated for 3 h at 37°C in 5% CO$_2$, at the end of which time the bacteria were aspirated from the upper wells, and cells were washed three times with PBS or HBSS. Fresh DMEM–F-12 with 1% mannose was added to the apical chamber, 100 μg/ml gentamicin was added to the apical and basolateral chambers, resistance was measured, and the cells were incubated for an additional 21 h. Resistance was taken at select intervals during this incubation.

Cell viability assay. The Live/Dead viability/cytotoxicity kit for mammalian cells from Molecular Probes (Invitrogen, Carlsbad, CA) was used to determine viability of cells. An infection was performed as described above, and cells were stained at the 24-h point as per the manufacturer's instructions. Dead (red) cells were enumerated using a Zeiss Axioskop microscope at ×63 magnification in 20 fields per Transwell.

Intestinal cell monolayer permeability assay. Polarized T84 cells were infected in triplicate with various bacterial strains for 3 h; after the infection, monolayers were washed and treated with gentamicin as described above. Eighteen hours later, P-buffer (23) containing either dextran conjugated to fluorescein isothiocyanate (FITC-dextran) or bovine serum albumin (BSA) conjugated to FITC (FITC-BSA) (Sigma) at 10 mg/ml was added to the apical side. P-buffer was added to the basolateral chambers. P-buffer containing EGTA at a concentration of 2 mM (23) was used in the apical chamber as a positive control. After 6 h of incubation with the FITC conjugates, fluorescence at 518 nm was measured in the basolateral compartment by using a Cary Eclipse fluorometer (Varian, Inc. Scientific Instruments).

Immunofluorescence staining of T84 cells. Twenty-four hours after a 3-h infection, T84 monolayers were rinsed three times with PBS and fixed for antibody staining. For staining with occludin and zonula occludens-1 (ZO-1), cells were first incubated with 0.2% Triton X-100–PBS on ice for 2 min and then fixed with 3% paraformaldehyde for 30 min at 4°C, followed by incubation with 0.05% Triton X-100–PBS for 5 min on ice. For claudin-1 staining, cells were fixed with ice-cold ethanol at −20°C for 20 min and then permeabilized with 1% Triton X-100 for 10 min at room temperature (RT). All cells were blocked in 5% normal goat serum (NGS)-PBS for 30 min at RT. Primary antibodies used were rabbit anti-occludin (1:100), mouse anti-ZO-1 (1:100), and rabbit anti-claudin-1 (1:25) (Invitrogen). Antibodies were diluted in 1% NGS-PBS and added to the cells for 1 h at RT. After three washes in PBS, secondary antibodies (goat anti-mouse Alexa 568 and goat anti-rabbit Alexa 488 at 1:500) (Invitrogen) were added in the same incubation solution along with 4′,6-diamidino-2-phenylindole (DAPI) for 1 h at RT. Cells were washed three times with PBS and once with water and then mounted using Vectashield hard-set mounting medium (Vector Laboratories). The images chosen were representative of the entire micrograph data set. Images were captured with a Zeiss LSM510 META laser-scanning confocal microscope in the Zeiss LSM510 software package, and figures were assembled in Adobe Photoshop 7.0.

Statistical analysis. Resistance data analysis, live/dead data analysis, paracellular permeability analysis, calculations of mean concentrations, standard deviations, and statistical analysis for this work were completed using Microsoft Excel and Graph-Pad Prism 3. One-way analysis of variance (ANOVA) multiple pairwise comparisons
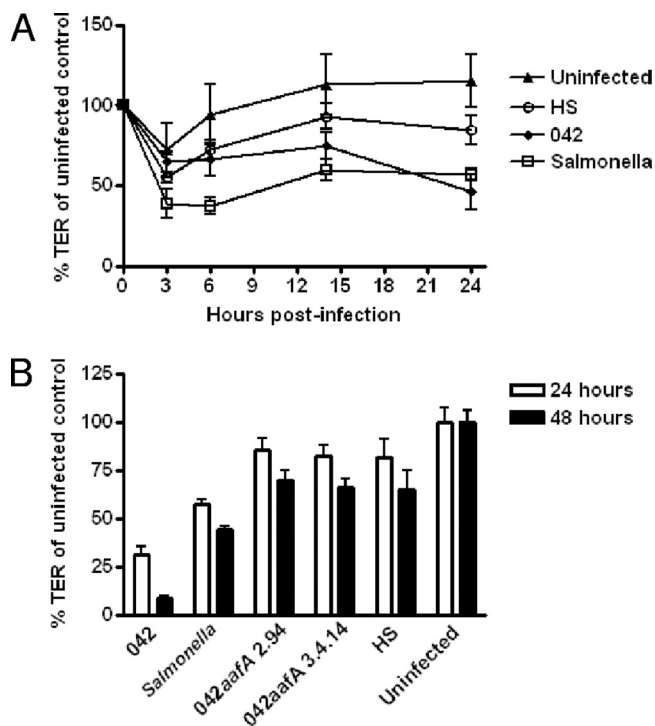
A

B

FIG. 1. EAEC induces barrier disruption. (A) Infection with EAEC 042 causes a time-dependent decrease in TER of polarized T84 monolayers. Polarized T84 cells were infected in EAEC strain 042; *Salmonella* Typhimurium served as positive control for barrier disruption, and commensal *E. coli* strain HS and uninfected monolayers served as negative controls. Three hours after the addition of bacteria, the infection was terminated by aspiration of the apical compartment medium and addition of fresh medium containing gentamicin. TER was measured at 0, 3, 6, 14, and 24 h after infection. The figure represents an average of five separate experiments with each performed in triplicate wells. Error bars indicate one standard deviation of mean TER. Strain 042 and *Salmonella* cells were significantly different from HS and uninfected T84 cells 24 h after infection ($P < 0.05$ determined by ANOVA). (B) EAEC strain 042 effects on epithelial permeability are irreversible over 48 h. Polarized T84 cells were infected in triplicate for 3 h, followed by treatment with gentamicin as described for panel A. White bars represent TER at 24 h, and black bars represent TER at 48 h after the 3-h infection. Strain 042 and *Salmonella* cell effects on TER were significantly different from that induced by HS, from uninfected monolayers, and from either 042*aafA* mutant at both 24 and 48 h. ∗, $P < 0.05$ determined by ANOVA with Tukey's posttest.

test with Tukey's and/or the Bonferroni posttest were used to determine statistical significance. The significant P value was set at $P < 0.05$.

RESULTS

EAEC strain 042 causes a persistent decrease in TER in polarized T84 intestinal epithelial cell monolayers. To characterize the effects of EAEC on intestinal barrier function, we measured the TER of polarized T84 intestinal epithelial cell monolayers infected with EAEC strain 042 for 3 h. At the conclusion of the infection period, the monolayers were washed and fresh medium containing gentamicin was added; TER was measured at intervals for an additional 21 h. We found no significant difference in TER between strain 042-infected monolayers and uninfected monolayers at the end of the 3-h infection period. However, over the ensuing period, TER diminished dramatically in monolayers infected with 042 (Fig. 1A). By 21 h postinfection, the reduction of
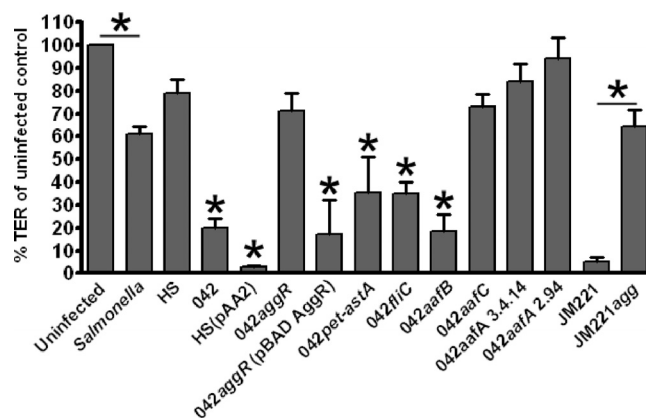

FIG. 2. Expression of the AAF/I adhesin by EAEC strain JM221 is necessary to elicit a decrease in TER in polarized T84 monolayers. Polarized T84 cells were infected for 3 h, and TER was compared with uninfected monolayers. TER measured at 24 h postinfection is represented as the percentage of TER in uninfected monolayers at this time point. Statistical significance in the mean of triplicate independent assays was determined with a one-way ANOVA, followed by Tukey's posttest. Asterisks indicate a significant difference from uninfected cells and HS at $P < 0.05$. TER after JM221 infection was significantly different from the TER of uninfected cells, HS-infected cells, and those infected with the JM221 AAF/I null mutant strain (JM221*agg*).

TER induced by 042 was statistically significant compared to uninfected monolayers and those infected with commensal *E. coli* strain HS. For a comparison, the reduction of TER induced by *Salmonella enterica* serovar Typhimurium strain CS401 was statistically significant compared to uninfected and HS-infected cells as early as 6 h postinfection.

The dramatic deterioration of TER over the 24-h observation period suggested that the effect induced by 042 may be more persistent than the effect induced by the enteropathogenic *E. coli* pathotype, which also affects T84 monolayer permeability (39). To address the duration of the EAEC-induced effect, we extended the observation period for an additional 24 h (48 h overall), exchanging the medium at the 24-h time point. We found that the TER of monolayers infected with strain 042 did not recover over 48 h postinfection (Fig. 1B).

Effect of EAEC on TER requires AggR and AafA, but not AafB. Commensal *E. coli* strain HS transformed with the 042 virulence plasmid pAA2 (15) induced diminution of TER indistinguishable from that of the wild-type parent, suggesting that pathogen-specific factors sufficient to account for the effects of EAEC on TER are encoded on the pAA2 virulence plasmid (Fig. 2). To further localize the genes involved in the phenotype, strains harboring mutations in all known plasmid-encoded putative virulence-related genes were assessed. Mutations in the genes encoding the Pet cytotoxin, the dispersin surface protein, and the cryptic Shf/Cap/VirK cluster (data not shown), as well as the chromosomally encoded flagellar protein FliC, induced the same level of TER reduction as did wild-type strain 042 (Fig. 2). HS harboring a pAA2 plasmid in which the genes encoding both the Pet and EAST1 toxins were deleted (HSΔ*pet-astA*) was also as potent as strain 042 in reducing TER (data not shown).

Since we had previously shown that the plasmid-encoded AAF/II adhesin in strain 042 was required for induction of IL-8 release from T84 monolayers (11), we tested two previously con-
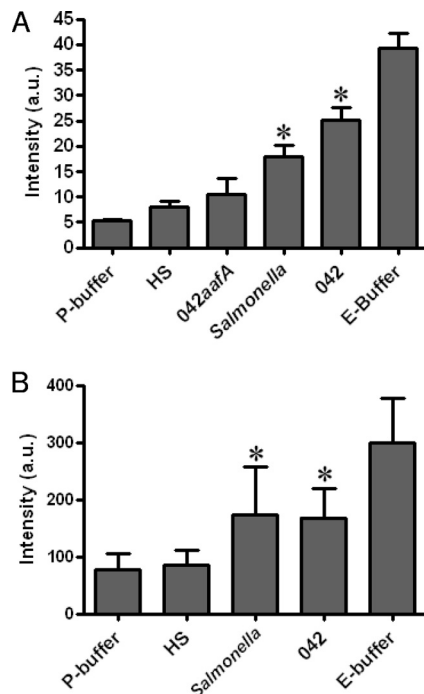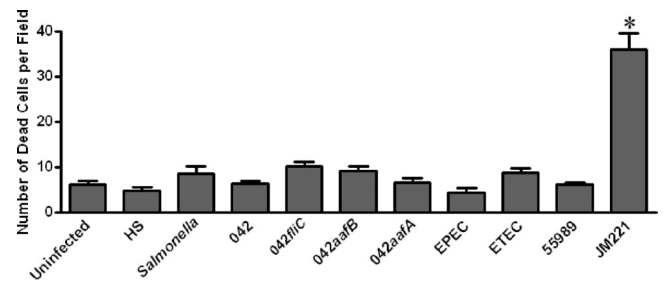
FIG. 4. Cell viability is unaffected by EAEC strain 042 infection but is significantly decreased after JM221 infection. Polarized T84 monolayers were infected for 3 h as described in legend to Fig. 1; at 24 h postinfection, cells were stained using the Live/Dead cell viability assay as described in Materials and Methods, and the number of dead (red) cells was enumerated by epifluorescence microscopy. Dead cells were counted in 20 fields at ×63 magnification from each well. Statistical significance was determined from a one-way ANOVA with Tukey's posttest. ∗, significant difference from HS and uninfected control ($P <$ 0.05).

FIG. 3. Infection with EAEC strain 042 increases paracellular permeability. Polarized T84 cells were infected for 3 h, and monolayers were washed and treated with gentamicin. At 18 h postinfection, cells were washed with PBS and P-buffer was added to the basolateral chamber; either FITC-BSA (A) or FITC-dextran (B) in P-buffer was added to the apical chamber at this time point. EGTA served as a positive control. At the 24-h time point, basolateral supernatants were sampled and analyzed using a fluorescence spectrophotometer. Statistical significance of triplicate assays was determined using one-way ANOVA followed by Tukey's posttest. ∗, significant difference from P-buffer and HS at $P < 0.01$.

structed strains with mutations of the major fimbrial protein AafA: 2.94, which produces defective AAF/II fimbriae, and 3.4.14, which does not produce any detectable AAF/II fimbriae. Neither mutant induced a significant reduction in TER compared to uninfected or HS-infected T84 cells. As predicted, mutations in the fimbrial usher protein AafC or the transcriptional activator AggR (required for AAF/II expression) were similarly unable to enhance barrier permeability. Complementation of 042aggR restored the ability of the strain to reduce TER.

The AAF fimbriae are comprised of the major pilin protein AafA and a minor pilin protein termed AafB. Whereas both mutations in major pilin protein AafA were unable to induce barrier permeability, a mutation in *aafB* did not alter the effect of 042 on TER (Fig. 2). These data suggest that the AAF/II fimbrial adhesins are necessary to cause TER reduction in infected cell monolayers, but that this effect does not require the protein AafB.

AAF/II is one of four described variants of the AAF adhesin. We found that the requirement for AAF/II in strain 042 also prevailed for AAF/I in a strain that expresses this variant: AAF/ I-encoding strain JM221 induced barrier dysfunction similar to that observed for strain 042, whereas JM221agg (deleted for the entire AAF/I gene cluster) did not cause reduction of TER. We recently described a very distantly related AAF, termed AAF/IV (3). In contrast to the strains expressing AAF/I and AAF/II,

AAF/IV-expressing EAEC strain C1010 did not affect TER in our system (data not shown).

EAEC-induced barrier disruption is a result of paracellular permeability. Reduction of TER may result either from disruption of tight junction integrity or from physiological modulation of ion flux (33). To assess barrier function directly, we studied monolayer permeability to FITC-conjugated dextran (molecular mass, 4 kDa) and FITC-conjugated BSA (67 kDa). These molecules were added to the apical chamber, and their ability to traverse the paracellular space was monitored by measuring fluorescence in the basolateral compartment. As a positive control for barrier disruption, we included an EGTA-containing buffer (E-buffer) and as a negative control the corresponding P-buffer, which contains the same ion concentration but lacks EGTA (23). As shown in Fig. 3, we observed augmented translocation of both FITC-dextran and FITC-BSA into the basolateral compartment after infection with 042, compared with HS or P-buffer, indicating increased permeability of molecules through the paracellular space after 042 infection. Strain 042aafA infection did not enhance the flux of FITC-labeled BSA, confirming that AAF/II is required to induce barrier permeability.

Cell viability is not affected by EAEC 042. One potential mechanism to account for the persistence of the EAEC effect on TER is cell death. To quantitate the number of nonviable cells in 042-infected T84 monolayers, we employed the fluorescent Live/ Dead viability/cytotoxicity kit assay, in which live cells appear green and nonviable cells red. Cells were infected for 3 h, and the assay was performed 21 h later. Dead cells were scored in blinded fashion using epifluorescence microscopy. We observed no significant differences between the number of dead T84 cells in monolayers infected with 042 compared with that of uninfected monolayers or those infected with strain HS (Fig. 4). In contrast, JM221-infected monolayers exhibited significantly higher numbers of dead cells than either 042-infected or uninfected monolayers. None of the other pathogenic strains (ETEC, EPEC, *Salmonella* sp., EAEC 55989) nor any of the 042 mutants induced significantly more cytotoxicity than the negative control strain HS. This suggests that cell death is not the cause of the decreased TER caused by EAEC 042.
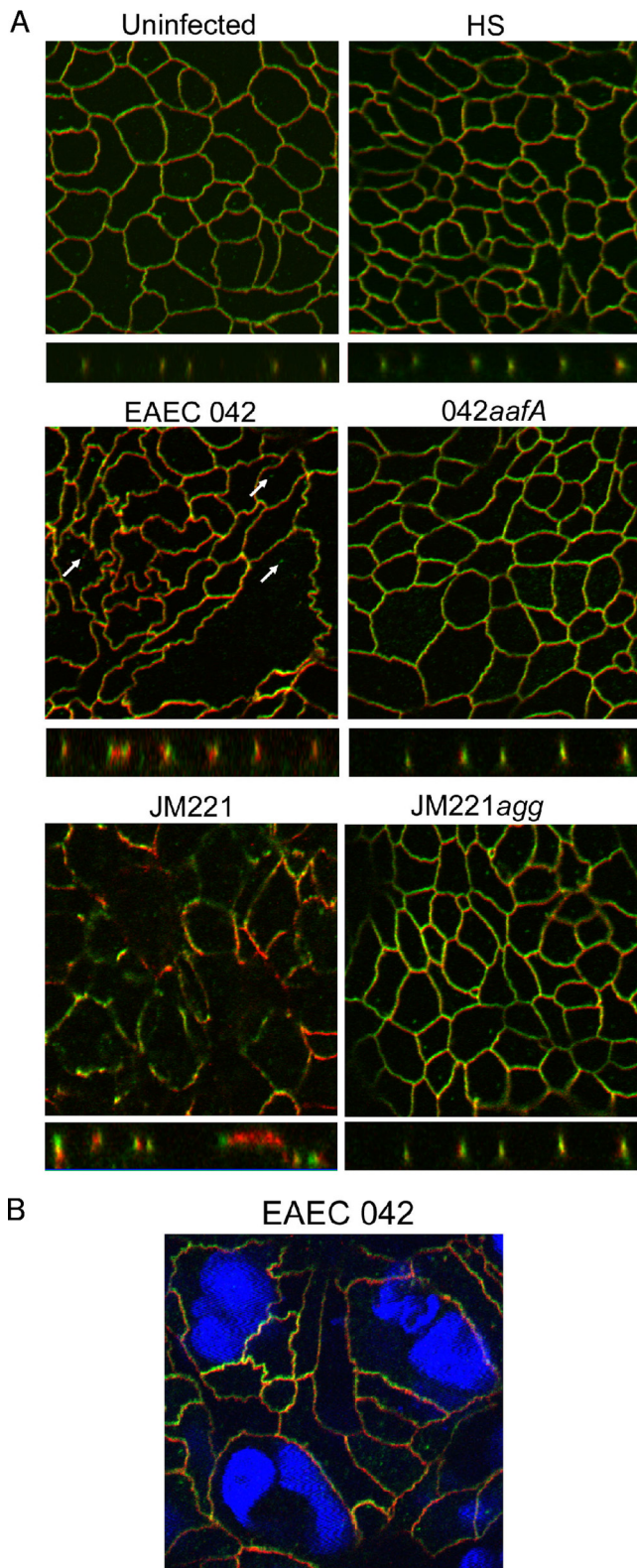
A

B

EAEC infection results in the redistribution of tight junction proteins and modification of cellular morphology. Because tight junction proteins regulate the traffic of molecules through the paracellular space, we hypothesized that the observed increases in paracellular permeability after EAEC infection would be accompanied by reorganization of tight junction proteins. We therefore assessed the localization of several tight junction proteins in monolayers infected with 042 and other EAEC strains. Infections were performed as previously described, and cells were labeled at 24 h postinfection. We focused these studies on the major structural components occludin, ZO-1, and claudin-1 (33), as localization of these proteins is frequently modified in instances of tight junction perturbation (4, 6, 12, 17, 29, 39).

Uninfected T84 cells displayed peripheral colocalization of occludin and ZO-1 (Fig. 5A), and cell edges were typically smooth and straight. Cells infected with commensal *E. coli* strain HS appeared similar to uninfected monolayers. In contrast, monolayers infected with strain 042 displayed jagged intercellular junctions when stained for ZO-1 or occludin (Fig. 5A). Although occludin and ZO-1 were largely colocalized, cytoplasmic vesicles containing occludin were observed in many cells (Fig. 5A). In addition, some cells appeared enlarged or elongated compared to uninfected cells. In some cases, the enlarged cells contained more than one nucleus, as observed with the DAPI stain, suggesting syncytium formation (Fig. 5B). Infection with the AAF/I-expressing strain JM221 caused distension of the cells and loss of the flat character of the monolayers, as well as a marked loss of occludin from the tight junctions. In contrast to 042-infected cells, JM221 cells maintained a regular shape with straight borders, although occludin and ZO-1 no longer colocalized. JM221*agg*-infected cells appeared normal (Fig. 5A).

ZO-1 physically interacts with phosphorylated tyrosine residues in the C-terminal tail of occludin in tight junctions (16, 33) and also binds to actin, providing stability to the epithelial layer (16). As noted above, cytoplasmic occludin-containing vesicles were observed in 042-infected monolayers. Analysis of the Z-plane images revealed dissociation of occludin and ZO-1 within the tight junctions as well, which was an effect that was not observed in HS-infected or 042*aafA*-infected monolayers. As with strain 042, ZO-1 and occludin appeared to be dissociated in cells infected with JM221. Infection with JM221*agg* did not alter occludin or ZO-1 localization (Fig. 5A).

The claudins act as principle regulators of cell monolayer TER by controlling the flux of ions through the paracellular pathway (33). A decrease in TER may be induced by claudin-1 disruption or downregulation (44). Claudin-1 has been shown to be aberrantly localized in response to infection by a variety of pathogens (13, 21, 44). We observed that monolayers infected with EAEC 042 or JM221 caused a dissociation of claudin-1 from the tight junctions (Fig. 6), whereas monolayers

FIG. 5. (A) AAF adhesins of EAEC strain 042 and JM221 contribute to the irregular morphology of T84 membranes and delocalization of occludin following infection. (A) After a 3-h infection, cells were stained with occludin (green) and ZO-1 (red). Images were acquired on a Zeiss LSM510 scanning confocal microscope at ×63 magnification. Z-sectioning was performed to visualize the association of occludin and ZO-1 in the tight junction plane. (B) EAEC 042 infection results in the formation of large multinucleate cells. Cells were stained for occludin (green), ZO-1 (red), and nuclei (DAPI) at 24 h postinfection, and images were captured with a Zeiss LSM510 scanning confocal microscope.
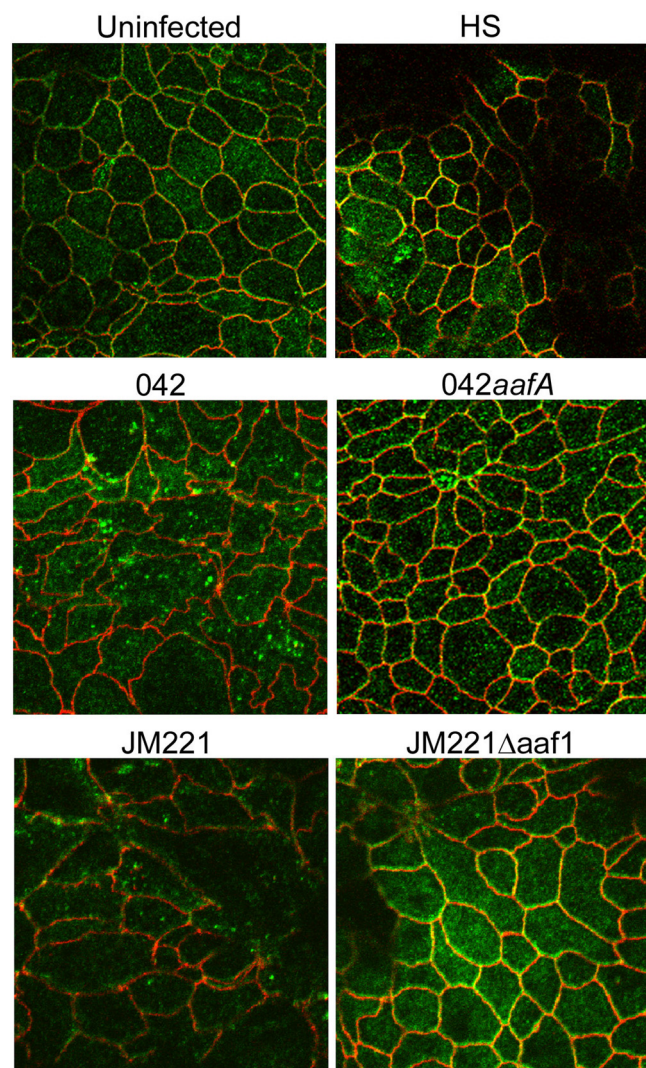
FIG. 6. Claudin-1 is lost from the tight junctions and found in cytoplasmic vesicles following infection with EAEC 042 and JM221. Cells were immunostained with anti-claudin-1 (green) and anti-ZO-1 (red) antibodies at 24 h postinfection. Images were obtained using a Zeiss LSM510 microscope.

infected with control strain HS appeared similar to uninfected cells. Neither 042aafA nor JM221aggA affected claudin-1 localization (Fig. 6).

DISCUSSION

Many enteric pathogens induce epithelial barrier disruption, although the mechanisms are diverse. We report here for the first time that infection of polarized T84 monolayers with the diarrheagenic *Escherichia coli* pathotype EAEC leads to a loss of barrier function. Permeability to a high-molecular-weight marker, FITC-BSA, suggests that the EAEC-induced barrier defect may be large enough to permit the leakage of proteins either from an apical to basolateral or basolateral to apical direction through the paracellular space. The former may permit penetration by bacterial toxins, or perhaps by the bacteria themselves, to basolateral receptors or the intestinal submu-

cosa. In addition, disruption of the epithelial fence may result in a loss of host ions and proteins into the lumen, which may exacerbate diarrheal disease or its long-term sequelae. The consequences of these pathogenic events warrant further investigation.

Immunofluorescence confocal microscopy demonstrated morphological changes in infected cells and delocalization of the tight junction proteins occludin and claudin-1 in response to EAEC infection. Internalization of occludin-containing blebs has been observed with other enteric pathogens, including *Clostridium perfringens* (40), *Campylobacter jejuni* (6), and EPEC (38). Though this phenotype has been seen accompanying alteration in intestinal barrier function, it has yet to be implicated as the direct mechanism of barrier impairment. Interestingly, occludin knockout mice do not manifest impaired epithelial permeability (32, 34), suggesting that internalization of occludin may be an epiphenomenon or a result of tight junction disruption. In contrast, claudins have been implicated as the "gatekeepers" of permeability (1, 43) and are capable of reconstituting tight junction strands in cells that do not normally form tight junctions (19). Therefore, loss of claudin-1 from the tight junctions in response to EAEC infections may have a major effect on permeability and barrier function. Involvement of claudin-1 is a common theme in enteric infection, as several pathogens, including *E. coli* C25, enterohemorrhagic *E. coli* 0157:H7 (45), *Arcobacter butzleri* (5), and *Salmonella enterica* serovar Typhimurium (18), cause redistribution of claudin-1 to some degree in addition to disrupting paracellular permeability.

We have shown that EAEC-induced barrier disruption of polarized T84 cells requires a functional AAF/I or AAF/II organelle, but not its minor fimbrial protein AafB. Though we have not yet shown that the AAF adhesins are sufficient to induce the complex effects we observe in EAEC infection, related organelles of the Dr family serve as invasins and cellular signaling agonists (2, 30, 36). Current investigations in our laboratory are focused on dissecting the potential direct effects of the AAF adhesins in the course of EAEC infection.

After a 3-h infection, we found that monolayers manifested low electrical resistance for up to 48 h, though cells were still viable at this time point. The life span of a mature enterocyte is typically 3 to 5 days, and therefore duration of the effect is likely to be most clinically relevant at the base of the intestinal crypts, where new cells are generated. Elucidating potential effects on the generation of new enterocytes and the resulting clinical implications will await studies in animal models.

REFERENCES

1. **Balkovetz, D. F.** 2006. Claudins at the gate: determinants of renal epithelial tight junction paracellular permeability. Am. J. Physiol. Renal Physiol. **290:** F572–F579.

2. **Bétis, F., P. Brest, V. Hofman, J. Guignot, I. Kansau, B. Rossi, A. Servin, and P. Hofman.** 2003. Afa/Dr diffusely adhering *Escherichia coli* infection in T84 cell monolayers induces increased neutrophil transepithelial migration, which in turn promotes cytokine-dependent upregulation of decay-accelerating factor (CD55), the receptor for Afa/Dr adhesins. Infect. Immun. **71:**1774–1783.

3. **Boisen, N., C. Struve, F. Scheutz, K. A. Krogfelt, and J. P. Nataro.** 2008. New adhesin of enteroaggregative Escherichia coli related to the Afa/Dr/AAF family. Infect. Immun. **76:**3281–3292.

4. **Boyle, E. C., N. F. Brown, and B. B. Finlay.** 2006. *Salmonella enterica* serovar Typhimurium effectors SopB, SopE, SopE2 and SipA disrupt tight junction structure and function. Cell. Microbiol. **8:**1946–1957.

5. **Bücker, R., H. Troeger, J. Kleer, M. Fromm, and J. D. Schulzke.** 2009. Arcobacter butzleri induces barrier dysfunction in intestinal HT-29/B6 cells. J. Infect. Dis. **200:**756–764.

6. **Chen, M. L., Z. Ge, J. G. Fox, and D. B. Schauer.** 2006. Disruption of tight junctions and induction of proinflammatory cytokine responses in colonic epithelial cells by Campylobacter jejuni. Infect. Immun. **74:**6581–6589.

7. **Czeczulin, J. R., S. Balepur, S. Hicks, A. Phillips, R. Hall, M. H. Kothary, F. Navarro-Garcia, and J. P. Nataro.** 1997. Aggregative adherence fimbria II, a second fimbrial antigen mediating aggregative adherence in enteroaggregative *Escherichia coli.* Infect. Immun. **65:**4135–4145.

8. **Derbise, A., B. Lesic, D. Dacheux, J. M. Ghigo, and E. Carniel.** 2003. A rapid and simple method for inactivating chromosomal genes in Yersinia. FEMS Immunol. Med. Microbiol. **38:**113–116.

9. **Donnenberg, M. S., and J. B. Kaper.** 1991. Construction of an eae deletion mutant of enteropathogenic Escherichia coli by using a positive-selection suicide vector. Infect. Immun. **59:**4310–4317.

10. **Dudley, E. G., C. Abe, J. M. Ghigo, P. Latour-Lambert, J. C. Hormazabal, and J. P. Nataro.** 2006. An IncI1 plasmid contributes to the adherence of the atypical enteroaggregative Escherichia coli strain C1096 to cultured cells and abiotic surfaces. Infect. Immun. **74:**2102–2114.

11. **Elias, W. P., Jr., J. R. Czeczulin, I. R. Henderson, L. R. Trabulsi, and J. P. Nataro.** 1999. Organization of biogenesis genes for aggregative adherence fimbria II defines a virulence gene cluster in enteroaggregative *Escherichia coli.* J. Bacteriol. **181:**1779–1785.

12. **Fedwick, J. P., T. K. Lapointe, J. B. Meddings, P. M. Sherman, and A. G. Buret.** 2005. *Helicobacter pylori* activates myosin light-chain kinase to disrupt claudin-4 and claudin-5 and increase epithelial permeability. Infect. Immun. **73:**7844–7852.

13. **Guttman, J. A., F. N. Samji, Y. Li, A. W. Vogl, and B. B. Finlay.** 2006. Evidence that tight junctions are disrupted due to intimate bacterial contact and not inflammation during attaching and effacing pathogen infection in vivo. Infect. Immun. **74:**6075–6084.

14. **Harrington, S. M., E. G. Dudley, and J. P. Nataro.** 2006. Pathogenesis of enteroaggregative *Escherichia coli* infection. FEMS Microbiol. Lett. **254:**12–18.

15. **Harrington, S. M., M. C. Strauman, C. M. Abe, and J. P. Nataro.** 2005. Aggregative adherence fimbriae contribute to the inflammatory response of epithelial cells infected with enteroaggregative *Escherichia coli.* Cell. Microbiol. **7:**1565–1578.

16. **Hecht, G. A.** 2003. Enteric pathogens that affect intestinal epithelial tight junctions, p. 285–300. *In* G. A. Hecht (ed.), Microbial pathogenesis and the intestinal epithelial cell. ASM Press, Washington, DC.

17. **Kim, J. Y., U. S. Sajjan, G. P. Krasan, and J. J. LiPuma.** 2005. Disruption of tight junctions during traversal of the respiratory epithelium by *Burkholderia cenocepacia.* Infect. Immun. **73:**7107–7112.

18. **Köhler, H., T. Sakaguchi, B. P. Hurley, B. A. Kase, H. C. Reinecker, and B. A. McCormick.** 2007. Salmonella enterica serovar Typhimurium regulates intercellular junction proteins and facilitates transepithelial neutrophil and bacterial passage. Am. J. Physiol. Gastrointest. Liver Physiol. **293:**G178–G187.

19. **Kubota, K., M. Furuse, H. Sasaki, N. Sonoda, K. Fujita, A. Nagafuchi, and S. Tsukita.** 1999. Ca(2+)-independent cell-adhesion activity of claudins, a family of integral membrane proteins localized at tight junctions. Curr. Biol. **9:**1035–1038.

20. **Levine, M. M., E. J. Bergquist, D. R. Nalin, D. H. Waterman, R. B. Hornick, C. R. Young, and S. Sotman.** 1978. Escherichia coli strains that cause diarrhoea but do not produce heat-labile or heat-stable enterotoxins and are non-invasive. Lancet **i:**1119–1122.

21. **Li, Q., Q. Zhang, C. Wang, X. Liu, N. Li, and J. Li.** 2009. Disruption of tight junctions during polymicrobial sepsis in vivo. J. Pathol. **218:**210–221.

22. **Ma, C., M. E. Wickham, J. A. Guttman, W. Deng, J. Walker, K. L. Madsen, K. Jacobson, W. A. Vogl, B. B. Finlay, and B. A. Vallance.** 2006. Citrobacter rodentium infection causes both mitochondrial dysfunction and intestinal epithelial barrier disruption in vivo: role of mitochondrial associated protein (Map). Cell. Microbiol. **8:**1669–1686.

23. **Matsuzawa, T., A. Kuwae, and A. Abe.** 2005. Enteropathogenic Escherichia coli type III effectors EspG and EspG2 alter epithelial paracellular permeability. Infect. Immun. **73:**6283–6289.

24. **Nataro, J. P.** 2004. Enteroaggregative *Escherichia coli,* p. 101–110. *In* W. M. Scheld, B. E. Murray, and J. M. Hughes (ed.), Emerging infections 6. ASM Press, Washington, DC.

25. **Nataro, J. P.** 2005. Enteroaggregative Escherichia coli pathogenesis. Curr. Opin. Gastroenterol. **21:**4–8.

26. **Nataro, J. P., Y. Deng, S. Cookson, A. Cravioto, S. J. Savarino, L. D. Guers, M. M. Levine, and C. O. Tacket.** 1995. Heterogeneity of enteroaggregative Escherichia coli virulence demonstrated in volunteers. J. Infect. Dis. **171:**465–468.

27. **Nataro, J. P., V. Mai, J. Johnson, W. C. Blackwelder, R. Heimer, S. Tirrell, S. C. Edberg, C. R. Braden, J. Glenn Morris, Jr., and J. M. Hirshon.** 2006. Diarrheagenic Escherichia coli infection in Baltimore, Maryland, and New Haven, Connecticut. Clin. Infect. Dis. **43:**402–407.

28. **Nataro, J. P., J. Seriwatana, A. Fasano, D. R. Maneval, L. D. Guers, F. Noriega, F. Dubovsky, M. M. Levine, and J. G. Morris, Jr.** 1995. Identification and cloning of a novel plasmid-encoded enterotoxin of enteroinvasive Escherichia coli and Shigella strains. Infect. Immun. **63:**4721–4728.

29. **Nusrat, A., C. von Eichel-Streiber, J. R. Turner, P. Verkade, J. L. Madara, and C. A. Parkos.** 2001. Clostridium difficile toxins disrupt epithelial barrier function by altering membrane microdomain localization of tight junction proteins. Infect. Immun. **69:**1329–1336.

30. **Peiffer, I., A. B. Blanc-Potard, M. F. Bernet-Camard, J. Guignot, A. Barbat, and A. L. Servin.** 2000. Afa/Dr diffusely adhering Escherichia coli C1845 infection promotes selective injuries in the junctional domain of polarized human intestinal Caco-2/TC7 cells. Infect. Immun. **68:**3431–3442.

31. **Rakeman, J. L., H. R. Bonifield, and S. I. Miller.** 1999. A HilA-independent pathway to Salmonella typhimurium invasion gene transcription. J. Bacteriol. **181:**3096–3104.

32. **Saitou, M., M. Furuse, H. Sasaki, J.-D. Schulzke, M. Fromm, H. Takano, T. Noda, and S. Tsukita.** 2000. Complex phenotype of mice lacking occludin, a component of tight junction strands. Mol. Biol. Cell **11:**4131–4142.

33. **Schneeberger, E. E., and R. D. Lynch.** 2004. The tight junction: a multifunctional complex. Am. J. Physiol. Cell Physiol. **286:**C1213–C1228.

34. **Schulzke, J. D., A. H. Gitter, J. Mankertz, S. Spiegel, U. Seidler, S. Amasheh, M. Saitou, S. Tsukita, and M. Fromm.** 2005. Epithelial transport and barrier function in occludin-deficient mice. Biochim. Biophys. Acta **1669:**34–42.

35. **Schulzke, J. D., S. Ploeger, M. Amasheh, A. Fromm, S. Zeissig, H. Troeger, J. Richter, C. Bojarski, M. Schumann, and M. Fromm.** 2009. Epithelial tight junctions in intestinal inflammation. Ann. N. Y. Acad. Sci. **1165:**294–300.

36. **Servin, A. L.** 2005. Pathogenesis of Afa/Dr diffusely adhering Escherichia coli. Clin. Microbiol. Rev. **18:**264–292.

37. **Sheikh, J., J. R. Czeczulin, S. Harrington, S. Hicks, I. R. Henderson, C. Le Bouguenec, P. Gounon, A. Phillips, and J. P. Nataro.** 2002. A novel dispersin protein in enteroaggregative Escherichia coli. J. Clin. Invest. **110:**1329–1337.

38. **Shifflett, D. E., D. R. Clayburgh, A. Koutsouris, J. R. Turner, and G. A. Hecht.** 2005. Enteropathogenic E. coli disrupts tight junction barrier function and structure in vivo. Lab. Invest. **85:**1308–1324.

39. **Simonovic, I., J. Rosenberg, A. Koutsouris, and G. Hecht.** 2000. Enteropathogenic Escherichia coli dephosphorylates and dissociates occludin from intestinal epithelial tight junctions. Cell. Microbiol. **2:**305–315.

40. **Singh, U., L. L. Mitic, E. U. Wieckowski, J. M. Anderson, and B. A. McClane.** 2001. Comparative biochemical and immunocytochemical studies reveal differences in the effects of Clostridium perfringens enterotoxin on polarized CaCo-2 cells versus Vero cells. J. Biol. Chem. **276:**33402–33412.

41. **Steiner, T. S., J. P. Nataro, C. E. Poteet-Smith, J. A. Smith, and R. L. Guerrant.** 2000. Enteroaggregative Escherichia coli expresses a novel flagellin that causes IL-8 release from intestinal epithelial cells. J. Clin. Invest. **105:**1769–1777.

42. **Struve, C., M. Bojer, and K. A. Krogfelt.** 2008. Characterization of Klebsiella pneumoniae type 1 fimbriae by detection of phase variation during colonization and infection and impact on virulence. Infect. Immun. **76:**4055–4065.

43. **Turksen, K., and T. C. Troy.** 2004. Barriers built on claudins. J. Cell Sci. **117:**2435–2447.

44. **Wei, X., Z. S. Jia, J. Q. Lian, Y. Zhang, J. Li, L. Ma, L. Ye, J. P. Wang, L. Pan, P. Z. Wang, and X. F. Bai.** 2009. Inhibition of hepatitis C virus infection by interferon-gamma through downregulating claudin-1. J. Interferon Cytokine Res. **29:**171–178.

45. **Zareie, M., J. Riff, K. Donato, D. M. McKay, M. H. Perdue, J. D. Soderholm, M. Karmali, M. B. Cohen, J. Hawkins, and P. M. Sherman.** 2005. Novel effects of the prototype translocating Escherichia coli, strain C25 on intestinal epithelial structure and barrier function. Cell. Microbiol. **7:**1782–1797.